Isotopic evidence (δ^{13}C, δ^{37}Cl, δ^2H) for distinct transformation mechanisms of chloroform: Catalyzed H$_2$-water system vs. zero-valent iron (ZVI)

Berhane Abrha Asfaw [a,*], Kaori Sakaguchi-Söder [a,b], Thomas Schiedek [a], Nils Michelsen [a], Anat Bernstein [c], Hagar Siebner [c], Christoph Schüth [a]

[a] *Institute of Applied Geosciences, Technische Universität Darmstadt, Schnittspahnstraße 9, 64287 Darmstadt, Germany*
[b] *Institut IWAR, Technische Universität Darmstadt, Franziska-Braun-Straße 7, 64287 Darmstadt, Germany*
[c] *Department of Environmental Hydrology and Microbiology, The Zuckerberg Institute for Water Research, Ben-Gurion University of the Negev, Sde Boker Campus, 84990 Beer-Sheva, Israel*

ARTICLE INFO

ABSTRACT

Catalytic hydrodechlorination is an efficient technology for degrading organochlorinated compounds, such as chloroform (CF), into harmless products. Compound-specific stable isotope analysis (CSIA) of multiple elements is widely used for the investigation of degradation mechanisms. Yet, its application in the study of catalytic hydrodechlorination is still limited. We have applied CSIA to derive chlorine, carbon, and hydrogen isotope enrichment factors (ε) during the degradation of CF over Pd/Al$_2$O$_3$ and over Rh/Al$_2$O$_3$. In addition, the enrichment factors for the same isotopes were derived for the reaction of CF with zero-valent iron (ZVI) for comparison. For the reactions of CF over Pd/Al$_2$O$_3$ and Rh/Al$_2$O$_3$, ε_C values (-21.9 ± 0.25 ‰ and -23.4 ± 2.3 ‰) and ε_{Cl} values (-12.1 ± 1.7 ‰ and -10.3 ± 0.6 ‰) were determined, respectively. The corresponding ε_C and ε_{Cl} values, for the dechlorination of CF with ZVI were -22.2 ± 2.8 ‰ and -4.7 ± 0.45 ‰, respectively. The apparent kinetic isotope effects (AKIE) of Cl suggest that the transformation mechanism in the catalyzed hydrogen-water system is a non-concerted reaction, unlike the known reductive dechlorination of CF with ZVI. Moreover, dual-isotope slopes ($\Lambda_{C/Cl}$) for both catalyzed reactions ($\Lambda_{Pd} = 1.8 \pm 0.13$ and $\Lambda_{Rh} = 2.1 \pm 0.14$) are markedly different than for the ZVI ($\Lambda_{ZVI} = 5.8 \pm 0.41$), reflecting that the reactions proceed in different mechanisms. For hydrogen isotopes, while there was no clear trend for the catalyzed reactions, an inverse secondary hydrogen isotope effect was observed for the reaction of CF with ZVI.

1. Introduction

Chloroform (CHCl$_3$, henceforth CF), a chlorinated organic compound having both natural and anthropogenic sources is widely spread in marine and terrestrial environments [1,2]. In the USA, it is one of the most commonly detected volatile organic compounds (VOCs) in groundwater [3]. It is environmentally toxic and ranks 11th in the 2019 substance priority list of the Agency for Toxic Substances and Disease Registry [4]. To humans, CF is potentially carcinogenic [5].

Chloroform is manufactured as an industrial solvent and it is a chemical intermediate and by-product of various processes [6–11]. It is also formed as a by-product during drinking- or pool-water chlorination, and during seawater or wastewater treatment as the chlorine (or its other forms, i.e. hypochlorite, hypochlorous acid, and chlorine dioxide) reacts with dissolved organic matter [12–21]. These various sources contribute to its ubiquitous occurrence in the environment and specifically in surface water and groundwater.

The efficiency of biotic and abiotic natural attenuation processes removing chlorinated organic compounds from the water phase under natural conditions is limited. Consequently, several remediation methods based on reductive dechlorination, using zero-valent iron (ZVI) [22–25], noble metal catalysts such as palladium (Pd) and rhodium (Rh) [26–29], or a combination of both [30–36], have been developed. In addition to the direct electron transfer on the ZVI surface for dechlorination, all methods use molecular hydrogen as the electron donor to convert the chlorinated organic compounds into non-chlorinated products. While corrosion of ZVI in the aqueous phase, in addition to the direct reduction, generates the hydrogen necessary for the reaction, hydrogen has to be added in the case of catalytic conversion reactions, typically by bubbling the gas into the water phase [37] or by diffusion of

pressurized hydrogen through e.g. hollow fibre membrane modules [38] or diffusion stones [39]. In electrochemical remediation, hydrogen can also be generated from electrolysis of water as demonstrated in various studies [40–43]. For CF dechlorination by nano-sized ZVI, Song et al. [44] reported that the role of the evolved hydrogen is insignificant. By contrast, a number of studies report a significant role of the hydrogen in reductive dechlorination of a number of organic compounds [25, 45–47].

These techniques have been applied in in-situ remediation of contaminated aquifers. Examples comprise the application of ZVI in permeable reactive barriers (PRBs)[22,23,48,49], the direct injection of nano-scale ZVI, or nano-scale Fe/Pd bimetallic particles, both with or without support materials, into aquifers [24,25,48,50–56]. Noble metal catalysts have also been implemented in in-borehole treatment techniques [30,31,57].

Reductive dechlorination of CF using ZVI is well known [58–64] and there is also extensive literature on the catalytic hydrodechlorination of CF over palladium, rhodium, and other catalysts, pure or on different supports, alone or bi-metallic, and both, in gas and liquid phase reactions [7,8,65–79]. Typically, those studies focus on the degradation in terms of the catalysts' activities, selectivities, the role of grain sizes and support materials, and on the long-term performance of the catalysts. The evidence for and the quantification of degradation reactions are then mainly based on observed concentration changes and on products formed. While these approaches are sufficient for well-controlled laboratory experiments, they are susceptible to errors in the field, e.g. due to sorption, diffusion, dispersion, or changes in flow paths [80,81].

Compound-specific isotope analysis (CSIA) is an additional tool that can be applied to quantify the progress of degradation reactions, independent of concentrations. This is due to the fact that bonds containing the heavier isotope are more stable compared to bonds containing the lighter isotope, leading to kinetic isotope fractionation during degradation. The related isotope enrichment factor (ε) can be obtained by applying the Rayleigh equation to degradation data [80,82]. If the initial isotopic composition of a compound as well as the enrichment factor of a reaction is known, the progress of a reaction can be studied by measuring the isotopic composition of the remaining compound. In addition, CSIA can be used as an environmental forensic tool to identify contaminant sources [83–88] or to reveal transformation pathways and mechanisms [80,87,89–93].

CSIA studies ranging from batch and column experiments in the laboratory to field investigations focussing on various compounds have been carried out. For example, the use of stable carbon- as well as chlorine-CSIA (C- and Cl-CSIA) during the reductive dechlorination of trichloroethene (TCE) and perchloroethylene (PCE) with granular ZVI as well as nano-scale ZVI was demonstrated [94–96]. For CF, its formation from chlorination [97] and its biodegradation by a *Dehalobacter strain* [98] was studied using C-CSIA.

Multi-element CSIA of a compound provides even more information, specifically on reaction mechanisms, as lately summarized in a review of multi-element (C, H, Cl, Br) studies for several halogenated hydrocarbons [99]. For CF, C- and Cl-CSIA were applied in ZVI degradation experiments with varying pH, and with two microbial strains to distinguish between abiotic and biotic degradation reactions [100,101]. Recently, the technique was applied to investigate CF dechlorination with a novel *Dehalobacter* strain [102].

Besides to the individual isotopic fractionation patterns, or enrichment factors, obtained from multi-element isotope data, slopes derived from dual-isotope plots (lambda, Λ) are becoming an established line of evidence to identify various (bio)chemical transformation mechanisms and pathways [90,91,99,100,102–112]. The dual-isotope slope Λ numerically expresses the relationship between fractionation extents in the two plotted elements and often reflects the reaction mechanism and conditions [99], or kinetics, i.e. steps preceding bond cleavage [113]. A summary of C-Cl isotope slopes ($\Lambda_{C/Cl}$) is provided in a review article [114]. The technique, particularly using C-Cl isotope data, was applied

to study TCE dechlorination with ZVI [106] and to investigate the natural attenuation of carbon tetrachloride (CT) and CF [101] to characterize and ascertain degradation pathways at a contaminated field site [100]. For CF, $\Lambda_{C/Cl}$ for persulfate oxidation and alkaline hydrolysis showed significantly different slopes compared to the reductive dechlorination of CF with ZVI.

Laboratory-determined ε values are often applied to field investigations to quantify reaction progress [80,82,115–117]. The majority of these studies focus on biological transformation reactions or on abiotic reactions, e.g. when using ZVI. Despite the potential of catalytic hydrodechlorination for remediation of contaminated groundwater, CSIA studies focussing on one or multiple elements are still scarce [45, 81]. In this study, we therefore performed batch experiments to (i) investigate and derive the stable C, Cl, and H isotope enrichment factors for chloroform during its catalytic reductive hydrodechlorination over Pd/Al_2O_3 and over Rh/Al_2O_3 in the water phase, and (ii) compare these enrichment factors with the ones obtained for the reductive dechlorination of chloroform using ZVI. We then generated dual-isotope plots to derive $\Lambda_{C/Cl}$ values for all reactions.

2. Materials and methods

2.1. Experimental setup and sample preparation

Chloroform (Sigma-Aldrich PHR1552), palladium on aluminum oxide powder (Pd/Al_2O_3, 10 wt. %; Sigma-Aldrich 440086), and rhodium on aluminum oxide powder (Rh/Al_2O_3, 5 wt. %; Sigma-Aldrich 212857) were purchased from Sigma-Aldrich/Merck (Darmstadt, Germany). A series of CF stock solutions was produced by diluting the original CF standard with methanol (>99.9 %; Carl Roth GmbH, Karlsruhe, Germany).

For the catalytic reductive hydrodechlorination of CF over palladium and over rhodium, a 100 mL borosilicate glass syringe (Poulten and Graf GmbH, Wertheim, Germany) was used as a reaction vessel. It was modified to allow sampling via a glass-sampling port capped with a Mininert valve (Alltech Grom GmbH, Rottenburg-Hailfingen, Germany) at the side of the syringe and placed vertically on a stirrer [118]. 100 mL deionized water was then filled into the syringe and saturated with H_2 gas by bubbling (approx. 0.8 mM). The plunger was inserted leaving no headspace by venting the excess gas through the sampling port. CF stock solution was injected through the sampling port to adjust a concentration of approx. 100 mg/L. To start the degradation reaction, either the Pd/Al_2O_3 (40 mg) or the Rh/Al_2O_3 (80 mg) was injected as slurry in deionized water through the sampling port.

From the reaction vessel different samples were taken. For carbon and hydrogen isotope analyses, water samples (1 mL) were withdrawn using a glass syringe with a syringe filter ($0.2\,\mu m$), and transferred into 2 mL glass vials with PTFE lined caps. For chlorine isotope analyses, $15\,\mu L$ of the water phase from each 1 mL sample were withdrawn and added to 10 mL deionized water in 20 mL headspace glass vials. A first set of water samples was taken prior to the injection of the catalyst to obtain the initial CF concentration. Changes in water volume in the reactor syringe due to sampling were adjusted by the movement of the glass plunger, thus avoiding any headspace.

To investigate the degradation of CF with ZVI, granular iron fillings obtained from Gotthart Maier GmbH (Rheinfelden, Germany) were used. The grain size ranges from 0.3 to 2 mm and it has a surface area of $0.87\,m^2/g$ (± 0.01) [119]. Two 120 mL glass vials with 200 g of ZVI and 50 mL of deionized water were prepared and capped with Mininert valves. One was used for analyzing carbon and hydrogen isotopes and the other one for analyzing chlorine isotopes. A third vial without iron served as the blank vial. CF stock solution was added to the vials to adjust a concentration of approx. 100 mg/L. Vials were covered with aluminum foil, kept on a horizontal shaker, and were sampled at experiment-specific intervals depending on reaction progress (SI, Appendix A3; Fig. A3.1 — Fig. A3.3).

For carbon and hydrogen isotope analyses, 1 mL water samples were taken from the respective vial and the reference vial and transferred into 2 mL glass vials with PTFE lined caps. For chlorine isotope analyses, 100 µL gas phase samples were taken from the respective vials and the reference vial. The gas phase samples were injected into 20 mL crimp top vials filled with 10 mL deionized water and closed with aluminum crimp caps.

2.2. Isotope and concentration analyses

To determine carbon and hydrogen stable isotope ratios in all experiments, the headspace in the 2 mL glass vials was sampled (20 – 500 µL) and directly injected into a gas chromatograph (Trace 1310, Thermo Fisher, Bremen, Germany) equipped with a flame ionization detector (FID) and connected through a combustion/pyrolysis interface to an isotope ratio mass spectrometer (IRMS; Delta V Advantage, Thermo Fisher). The IRMS was equipped with a triple collector for CO_2 (m/z = 44, 45, 46) and a dual collector for H_2 (m/z = 2, 3). Method details can be found in the Supplementary information (SI, Appendix A1).

Stable chlorine isotopes were determined using the 20 mL headspace glass vials and a purge and trap (P&T) system (PTA 3000; IMT, Vohenstrauß, Germany) coupled to a gas chromatograph with a quadrupole mass spectrometer (P&T-GC-qMS, Agilent GC 6890/5973MSD) [96,120] in the selected ion mode (SIM). Analyzed masses were m/z 83 and 85. GC-qMS runs were also used to determine chloroform concentrations, and to detect reaction intermediates. More details are available (SI, Appendix A2).

Linearity ranges for CF and the corresponding isotopes using P&T-GC-qMS and IRMS were checked before the experiments. Repeated measurements of various concentrations of the in-house CF standard, covering the concentration range of the samples from the experiments, revealed an overall precision better than 0.4 ‰, 0.4 ‰, and 6 ‰ for $\delta^{13}C$, $\delta^{37}Cl$, and δ^2H, respectively. Lower limits of quantification for C- and H-CSIA were about 7.1 and 3.93 ng on-column mass of carbon and hydrogen, respectively (more details in the SI, Appendix A4). For chlorine, the lower limit of quantification was about 267.4 ng Cl on-column achieved from a 30 µg/L concentration of CF in 10 mL deionized water. An aqueous CF concentration of 43.5 mg/L and 30 mg/L, when 100 µL head space is injected under the experimental conditions we reported in this work, would give the minimum sample amount for the linearity range of C- and H-CSIA, respectively.

2.3. Isotope data evaluation

The isotope ratios are expressed using the delta notation ($\delta^{13}C$, $\delta^{37}Cl$, and δ^2H) (Eq. 1)

$$\delta_{sample}\ ‰ = \left[\frac{R_{Sample} - R_{Reference}}{R_{Reference}}\right] * 1000 \tag{1}$$

where R_{sample} and $R_{Reference}$ are the isotope ratios of CF in the sample and reference standard, respectively [121]. Due to a lack of an isotopically defined reference material for CF, an in-house CF standard was used. Hence, the isotope values reported are not absolute numbers but reflect the changes as the reaction proceeds. Therefore, the first obtained isotopic values in the reference vials were set to 0 ‰.

To determine the bulk isotope enrichment factor ε [‰] of CF, a modified version of the Rayleigh equation [82] was applied for $\delta^{13}C$, $\delta^{37}Cl$, and δ^2H (Eq. 2):

$$\varepsilon‰ = \frac{1000 * \ln(\frac{\delta_t + 1000}{\delta_0 + 1000})}{\ln f} \tag{2}$$

where δ_0 and δ_t are the isotopic composition of CF at the beginning and at time t, respectively. f is the remaining fraction of CF during the dechlorination reaction, calculated as the quotient of the concentration at time t and the initial concentration (C_t/C_0). As the reductive

dechlorination of CF with ZVI was performed in vials with headspace, the concentration at any time t was corrected to account for the mass of CF removed during sampling, and also accounting for the change in the ratio between water phase and gas phase, as CF is a volatile compound [122].

The apparent kinetic isotope effect (AKIE) was calculated according to Eq. 3 [82,100]:

$$AKIE = \frac{1}{1 + \left(\frac{z*n}{x} - \varepsilon bulk\right)} \tag{3}$$

where n is the number of atoms of the considered element in the molecule, x is the number of these atoms located at a reactive site, and z is the number of atoms located at reactive sites that are in intramolecular competition.

For the evaluation of the dual-isotope plots and to determine the slope of the correlation between $\delta^{13}C$ and $\delta^{37}Cl$ ($\Lambda_{C/Cl}$), the York method of regression [123] adapted to RStudio [124], was applied as suggested in Ojeda et al. [104] for such plots.

3. Results and discussion

3.1. CF transformation and associated Isotope effects

Concentration data showed that CF dechlorination reactions over Pd/Al_2O_3, Rh/Al_2O_3, and with ZVI followed first-order kinetics, with much faster degradation for the two noble metals compared to the ZVI, as expected (SI, Fig. A3.1 — Fig. A3.3). Rates were highest for the Pd/Al_2O_3 catalyst. In all reactions, dichloromethane and chloromethane were observed as intermediate products in low concentrations, especially in the catalyzed reactions, and methane was the final product. Intermediate products and methane were not quantified or isotopically characterized.

Fig. 1 presents the Rayleigh plots for the isotopic changes of C, Cl, and H during the reactions and Table 1 shows the resulting enrichment factors ε (‰), the apparent kinetic isotope effects AKIE (-), and the slopes of the dual-isotope plots ($\Lambda_{C/Cl}$).

Concerning C, for the Pd and Rh catalysts as well as for the ZVI, very similar enrichment factors were determined (-21.9 ± 0.25 ‰, -23.4 ± 2.3 ‰, and -22.2 ± 2.8 ‰, respectively, Fig. 1: A, D, and G). These values are in line with reported carbon enrichment factors for reductive dechlorination of CF using ZVI (-33 ± 11 ‰ [100], and -20 ± 9 ‰ [125]) with significantly better precisions. For the catalyzed hydrodechlorination of CF, no C-isotope enrichment factors are reported so far.

For Cl, the enrichment factors for the two noble metal catalysts were similar (-12.1 ± 1.7 ‰ and -10.3 ± 0.6 ‰ for Pd/Al_2O_3 and Rh/Al_2O_3, respectively, Fig. 1: B and E), but higher than for the ZVI (-4.7 ± 0.45 ‰, Fig. 1: H). Our enrichment factor for the ZVI reductive dechlorination reaction is slightly higher than previously published results (-3 ± 1, -2 ± 1) [100,125]. For the catalyzed reactions, however, no fractionation factors are reported in the literature.

In case of hydrogen, the two catalysts and the ZVI showed different patterns. For Pd/Al_2O_3 and Rh/Al_2O_3, no clear unidirectional trends in δ^2H values were observed (Fig. 1: C and F, respectively). However, while for Pd/Al_2O_3 the hydrogen isotopes did not significantly change over the course of the experiment, large changes in the δ^2H values were observed for Rh/Al_2O_3 with an initial enrichment of heavier isotopes and a later depletion. Since no meaningful correlation between the concentration and hydrogen isotope values were observed (Fig. 1: C, and F), the enrichment factors were not calculated. For the ZVI, an inverse secondary hydrogen isotope effect with an enrichment factor of 28.7 ± 2.5 ‰ was recorded (Fig. 1: I).

Our results for the catalysts may suggest that CF is adsorbed to the catalyst surfaces through the Cl- or H- atoms and a certain extent of hydrogen isotope exchange is possible, as discussed in Chen et al. [74]
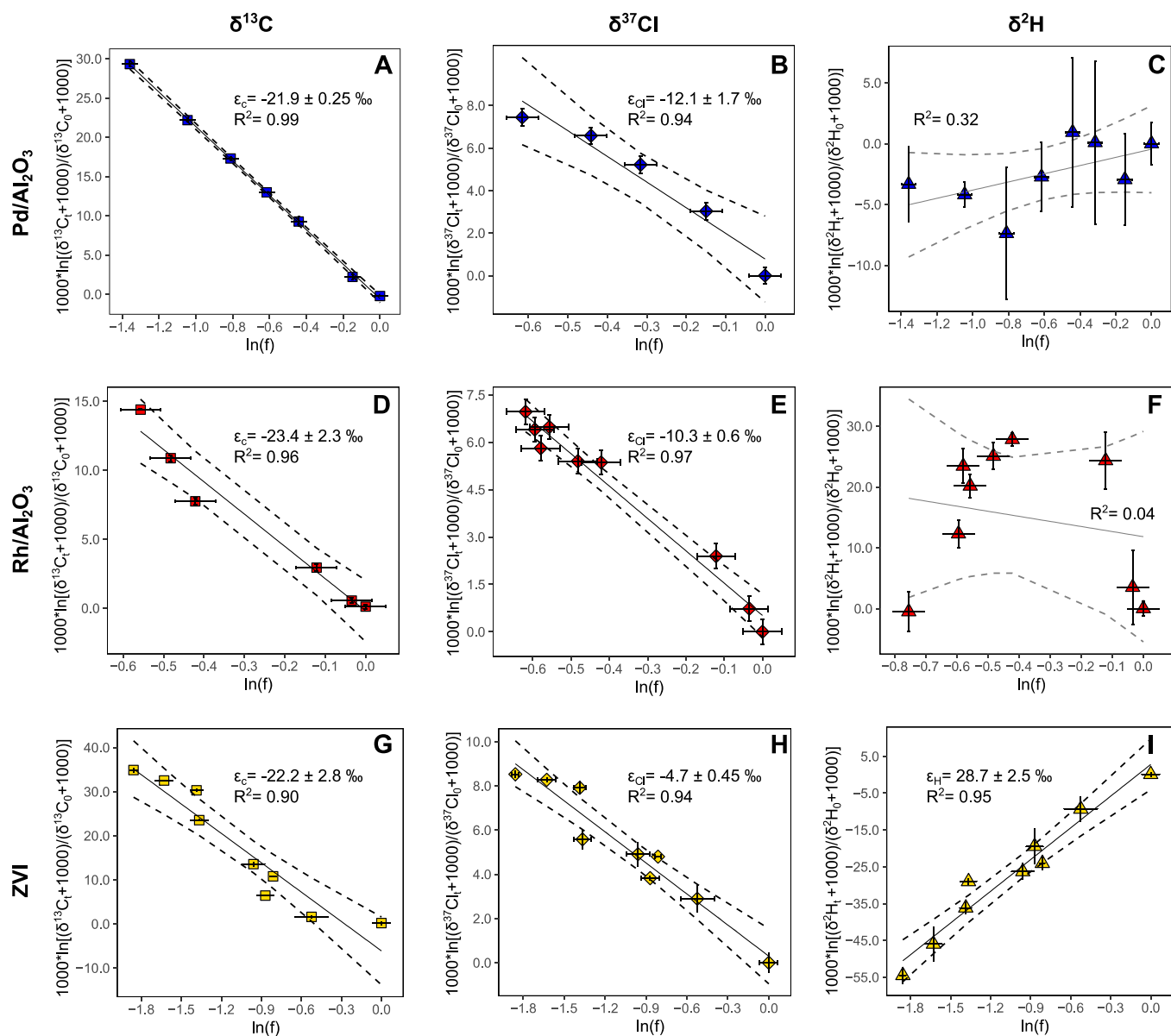
Fig. 1. Rayleigh isotope plots for the catalytic hydrodechlorination of CF over Pd/Al_2O_3 (A to C), Rh/Al_2O_3 (D to F), and dechlorination with ZVI (G to I). Dashed lines represent the 95 % confidence interval; vertical error bars represent uncertainty of the method (maximum 0.4 ‰ for C, 0.4 ‰ for Cl, and 6 ‰ for H) and horizontal error bars show uncertainty in concentration measurement. The slopes define ε in ‰. The hydrogen isotope enrichment factors ($ε_H$) for the catalyzed reactions were not calculated since the hydrogen isotope data show no meaningful correlation, as indicated by the low R^2 values (C and F) based on the Rayleigh model. Different f ranges are shown due to differing linearity ranges of the instruments for C-, Cl- and, H-CSIA (depending on temporal changes in instrument performance).

Table 1

C, Cl, and H isotope enrichment factors and dual-isotope slope ($Λ_{C/Cl}$) values obtained during degradation of CF over Pd/Al_2O_3, Rh/Al_2O_3, and with ZVI.

	Carbon			Chlorine			Hydrogen			2D
CF over	$ε_C$ [‰]	R^2	$AKIE_C$ [-]	$ε_{Cl}$ [‰]	R^2	$AKIE_{Cl}$ [-]	$ε_H$ [‰]	R^2	$AKIE_H$ [-]	$Λ_{C/Cl}$ [-]* *
Pd/Al_2O_3	−21.9 ± 0.25	0.99	1.0224 ± 0.0003	−12.1 ± 1.7	0.94	1.038 ± 0.0017*	* **	0.32	* **	1.8 ± 0.13
Rh/Al_2O_3	−23.4 ± 2.3	0.96	1.0240 ± 0.0023	−10.3 ± 0.6	0.97	1.032 ± 0.0006*	* **	0.04	* **	2.1 ± 0.14
ZVI	−22.2 ± 2.8	0.90	1.0227 ± 0.0028	−4.7 ± 0.45	0.94	1.014 ± 0.0005	28.7 ± 2.5	0.95	0.9721 ± 0.003	5.8 ± 0.41

* When concerted bond-cleavage is assumed (scenario 1, see Section 3.2).

** The $Λ_{C/Cl}$ values are derived from the dual-isotope slope shown in Fig. 2.

*** The hydrogen isotope data of the catalyzed reactions show no meaningful correlation, as indicated by the low R^2 values in Fig. 1 and this Table, and therefore do not fit to the Rayleigh model.

for Pd. In the exchange, either the hydrogen adsorbed to the catalyst surface or the hydrogen in the water molecule could be involved. Even though thermodynamically less expected, as Xu et al. [8] reported a C–H

bond of CF can be broken on Pd-surfaces to form CCl_3 radicals, which could result in an isotope fractionation. Moreover, superimposition of both equilibrium and kinetic isotope effects, as observed by Löffler et al.
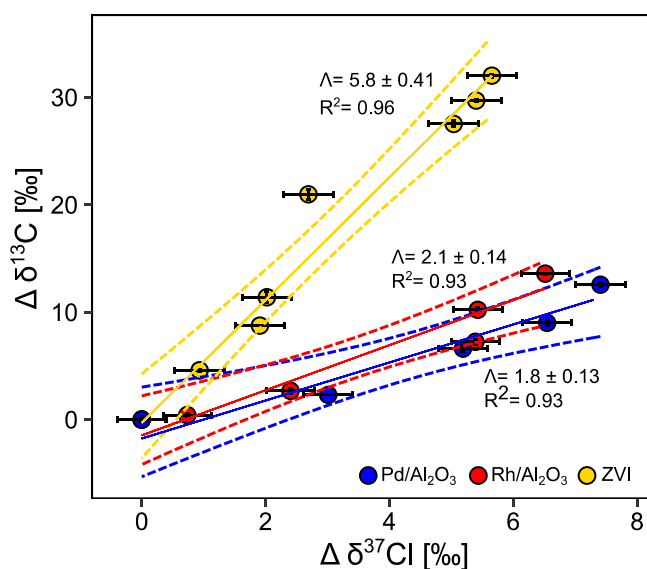
[126] in a hydrogenase reaction, might also contribute to the hydrogen isotope data scatter we observed.

In the case of ZVI, a similar hydrogen enrichment factor compared to ours (28.7 ± 2.5 ‰) was observed during the microbial reductive dechlorination of TCE ($\varepsilon_H = 34 \pm 11$ ‰) [127] and Van Breukelen et al. [128] modelled such an inverse isotope effect of hydrogen. These effects were attributed to nucleophilic addition reaction mechanisms. During the hydrodechlorination of CF with ZVI, a single C-Cl bond cleavage occurs in the first reaction step. Therefore, no primary H isotope effect is likely for this pathway and the measured ε_H indicates a secondary isotope effect in the H-atom located adjacent to the carbon in the reacting bond (C-Cl). This is in line with Elsner et al. [82] who suggested that breaking of a C-Cl bond could result in a secondary hydrogen isotope effect. Additional reaction pathways such as dehydrogenation mechanisms (CCl_3 formation) could also be possible reasons for inverse hydrogen isotope effects. On the contrary, there could be an additional isotope effect from repeated sample extraction where more headspace created in the vial might have led to a water-air partitioning isotope effect. Rostkowski et al. [129] and Horst and Lacrampe-Couloume [130] have obtained small but inverse hydrogen isotope effects for CF during volatilization from water.

The potentially combined processes occurring for the catalysts as well as for the ZVI might affect the overall fractionation, complicating a mechanistic interpretation of the results. Further experiments with e.g. deuterated CF and H_2O as well as volatilization experiments might provide additional evidence.

3.2. Comparison of the isotope effects and mechanism of dechlorination

To evaluate the reaction mechanisms, dual-isotope plots (changes in isotope values of C vs Cl) of the fractionation patterns were generated (Fig. 2). To avoid regression bias in both axes, the York method of regression, as suggested by Ojeda et al. [104], was used. For the dechlorination reaction with ZVI, a slope of 5.8 ± 0.41 was calculated, compared to previously reported $\Lambda_{C/Cl}$ values of 8 ± 2 [100], 8 ± 1 [125], 8 ± 1.4, and 8.1 ± 1.3 [131]. Our slightly attenuated slope is still

in the uncertainty range of some of the reported $\Lambda_{C/Cl}$ values for ZVI. Moreover, statistically there is no significant difference in the slope for the reactions with ZVI, as a p-value of 0.298 is calculated (t-test) for the $\Lambda_{C/Cl}$ reported in Torrentó et al. [100] and this work.

In contrast, a significant difference in $\Lambda_{C/Cl}$ between the ZVI-mediated and the catalyzed reactions was determined. While the $\Lambda_{C/Cl}$ for the catalytic hydrodechlorination reactions of CF over Pd/Al_2O_3 and over Rh/Al_2O_3 were 1.8 ± 0.13 and 2.1 ± 0.14, respectively (Fig. 2), the $\Lambda_{C/Cl}$ for ZVI was 5.8 ± 0.41. Comparing the regression lines of this study statistically, using covariance, there is no significant difference for the catalytic reactions, as a p-value of 0.419 is determined between both, Pd/Al_2O_3 and Rh/Al_2O_3 mediated reactions, whereas a p-value of < 0.001 is obtained for the catalytic reactions versus the ZVI reaction. We therefore assume different reaction mechanisms for the ZVI-based reaction and the catalytic ones as also deduced from the AKIE values, further discussed in the next paragraphs.

The isotope fractionation is a response to the underlying kinetic isotope effect (KIE) as degradation proceeds [82,87]. The calculated $AKIE_C$ values for all our reactions (1.0224 ± 0.0003 for Pd/Al_2O_3 catalysis, 1.0240 ± 0.0023 for Rh/Al_2O_3 catalysis, and 1.0227 ± 0.0028 for ZVI) are within the theoretical Streitwieser limit for C-Cl bond cleavage ($KIE_C = 1.057$) [82] and the rate-limiting step in the reactions is the cleavage of the C-Cl bond. In case of C and H, n, x, and z (see Section 2.3) are set to 1, as there is only one atom of each present in the CF molecule.

In CF, the Cl atoms are 3 ($n = 3$) whereas x and z are subject to the reaction mechanism. As a scenario 1, assuming all three chlorine atoms in CF are reacting in a concerted way (n, x and z, all 3), the $AKIE_{Cl}$ values were calculated for the CF dechlorination with ZVI (1.014 ± 0.0005) and for the Pd and Rh catalyzed reactions (1.038 ± 0.0017 and 1.032 ± 0.0006, respectively). The KIE_{Cl} for ZVI is near the expected maximum limit ($KIE_{Cl} = 1.013$) [82]. The values for the catalyzed reactions are however higher than the KIE_{Cl} theoretical limit for C-Cl bond cleavage. The high observed $AKIE_{Cl}$ for CF during catalyzed hydrodechlorination over Pd/Al_2O_3 and over Rh/Al_2O_3 might indicate that no intramolecular competition among the three chlorine atoms exists.

If we assume that no intramolecular competition occurs among the three chlorine atoms and stepwise bond-cleavage of the chlorine atoms occurs (scenario 2; both n and $x = 3$, and $z = 1$), re-evaluating the $AKIE_{Cl}$ results in values that are well within the Streitwieser limit, i.e. 1.012 ± 0.0017 for Pd/Al_2O_3 and 1.010 ± 0.0006 for Rh/Al_2O_3. According to Xu et al. [8] and Chen et al. [74], the chlorine end of the C-Cl bond, is mainly involved in the adsorption to the Pd surface. There are indeed three indistinguishable reactive sites, but our results also showed one chlorine atom at a time cleaves in the transition state. Hence, it is not a surprise in our case to observe a very large chlorine isotope effect for the Pd/Al_2O_3 catalyzed reaction. We consider the same phenomenon for the Rh/Al_2O_3 catalyzed reaction.

With regard to pathway, for the dechlorination of CF with ZVI hydrogenolysis and/or reductive elimination is suggested [100,125]. For the catalytic reactions both Pd/Al_2O_3 and Rh/Al_2O_3 mediated reactions show similar prominent carbon and chlorine isotope fractionation and comparable dual-isotope trends, likely evidencing a common reaction mechanism and/or the same pathway. We endorse dechlorination followed by the hydrogenation pathway, in line with other studies [8,28,77,79].

4. Conclusions

This study has explored isotope fractionation patterns during the catalytic hydrodechlorination of CF over Pd/Al_2O_3 and over Rh/Al_2O_3. The catalyzed reactions, also promoted in a broad range of fields [132, 133] were more rapid and effective than ZVI. In addition, CSIA of CF reductive dechlorination with ZVI has been investigated. Triple (chlorine, carbon, and hydrogen) isotope enrichment factors have been determined for the transformation reactions of CF where possible.

Fig. 2. Dual C-Cl isotope plots ($\Lambda_{C/Cl}$), i.e. changes in carbon versus chlorine isotope values, for chloroform during a catalytic hydrodechlorination over Pd/Al_2O_3 (blue circles), Rh/Al_2O_3 (red circles), and its reductive dechlorination with ZVI (golden circles). Solid lines correspond to the York regression and dashed lines show the 95 % confidence interval. Vertical error bars indicate uncertainty for duplicate measurements; horizontal error bars show a maximum uncertainty of 0.4 ‰ considered for duplicate chlorine isotopes. In some cases, the error bars are within symbol size.

All reactions resulted in a degradation of CF. During the reactions, there was similar C isotope fractionation for all three materials. In terms of Cl isotope, for the catalytic reactions over Pd/Al$_2$O$_3$ and over Rh/Al$_2$O$_3$, the ε_{Cl} values were similar, but significantly different compared to CF dechlorination with ZVI. In case of H isotope, there was no systematic fractionation for the catalyzed reactions, but a significant inverse secondary isotope effect was observed for the reaction with ZVI. Further experiments with deuterated CF and/or H$_2$O are required for additional insights into the reaction mechanisms.

Using dual-isotope slopes, $\Lambda_{C/Cl}$, distinct fractionation patterns attributed to transformation mechanism and/or pathway of CF have been revealed. We propose that the primary cause of the observed chlorine isotope effects for the catalytic reactions could be the absence of intramolecular competition; unlike during the dechlorination of CF with ZVI where there is competition (concerted reaction) among the chlorine atoms. Therefore, chlorine isotope measurements of CF could be a powerful monitoring tool in remediation studies, complementing concentration and carbon isotope analysis. This applies particularly to interventions using Pd, Rh, ZVI, or combinations thereof.

CRediT authorship contribution statement

Berhane Abrha Asfaw: Methodology, Investigation, Data Curation, Formal analysis, Software, Visualization, Writing – Original Draft. **Kaori Sakaguchi-Söder:** Conceptualization, Methodology, Data Curation, Software, Formal analysis, Validation, Writing – Review & Editing. **Thomas Schiedek**: Resources, Writing – Review & Editing. **Nils Michelsen**: Visualization, Writing – Review & Editing. **Anat Bernstein**: Writing – Review & Editing, Funding acquisition. **Hagar Siebner:** Writing – Review & Editing. **Christoph Schüth:** Conceptualization, Methodology, Resources, Validation, Writing – Review & Editing, Funding acquisition.

Declaration of Competing Interest

The authors declare that they have no known competing financial interests or personal relationships that could have appeared to influence the work reported in this paper.

Data Availability

Data will be made available on request.

Acknowledgments

Appendix A. Supporting information

Supplementary data associated with this article can be found in the online version at doi:10.1016/j.jece.2023.110005.

References

[1] F. Laturnus, K.F. Haselmann, T. Borch, C. Grøn, Terrestrial natural sources of trichloromethane (chloroform, CHCl3) - an overview, Biogeochemistry 60 (2002) 121–139, https://doi.org/10.1023/A:1019887505651.

[2] A. McCulloch, Chloroform in the environment: Occurrence, sources, sinks and effects, Chemosphere 50 (2003) 1291–1308, https://doi.org/10.1016/S0045-6535(02)00697-5.

[3] T. Ivannenko, J.S. Zogorski, Sources and occurrence of chloroform and other trihalomethanes in drinking-water supply wells in the United States, 1986 – 2001, U.S. Geol. Surv. Sci. Investig. Rep. 2006–5015. (2006) 13. https://pubs.usgs.gov/sir/2006/5015/sir2006–5015.pdf.

[4] Agency for toxic substances and disease registry(ATSDR). 2019 Substance Priority list, (n.d.). https://www.atsdr.cdc.gov/spl/index.html#2019spl.

[5] USEPA IRIS, Chloroform (CASRN 67–66-3), Integr. Risk Inf. Syst. (1999) 1–39. https://iris.epa.gov/static/pdfs/0025_summary.pdf.

[6] J. Estévez, E. Vilanova, Chloroform, Encycl. Toxicol. Third Ed. 1 (2014) 885–890. https://doi.org/10.1016/B978–0-12–386454-3.00479–6.

[7] M.A. Álvarez-Montero, M. Martin-Martinez, L.M. Gómez-Sainero, A. Arevalo-Bastante, J. Bedia, J.J. Rodriguez, Kinetic study of the hydrodechlorination of chloromethanes with activated-carbon-supported metallic catalysts, Ind. Eng. Chem. Res. 54 (2015) 2023–2029, https://doi.org/10.1021/ie5042484.

[8] L. Xu, S. Bhandari, J. Chen, J. Glasgow, M. Mavrikakis, Chloroform hydrodechlorination on palladium surfaces: a comparative DFT study on Pd(111), Pd(100), and Pd(211), Top. Catal. 63 (2020) 762–776, https://doi.org/10.1007/s11244-019-01218-6.

[9] S. Juuti, T. Vartiainen, P. Joutsenoja, J. Ruuskanena, Volatile organochlorine compounds formed in the bleaching of pulp with ClO2, Chemosphere 33 (1996) 437–448, https://doi.org/10.1016/0045-6535(96)00208-1.

[10] M.L. Aucott, A. McCulloch, T.E. Graedel, G. Kleiman, P. Midgley, Y.F. Li, Anthropogenic emissions of trichloromethane (chloroform, CHCl3) and chlorodifluoromethane (HCFC-22): Reactive chlorine emissions inventory, J. Geophys. Res. Atmos. 104 (1999) 8405–8415, https://doi.org/10.1029/1999JD900053.

[11] W.B. Mills, C.S. Lew, J.Y. Loh, Predictions of potential human health and ecological risks from power plant discharges of total residual chlorine and chloroform into rivers, Environ. Sci. Technol. 32 (1998) 2162–2171, https://doi.org/10.1021/es970209l.

[12] J.J. Rook, Haloforms in drinking water, J. Am. Water Work. Assoc. 68 (1976) 168–172, https://doi.org/10.1002/j.1551-8833.1976.tb02376.x.

[13] A. Bernstein, R. Studny, V. Shyntychea, D. Kurtzman, Y. Ganot, Y. Katz, B. A. Asfaw, K. Sakaguchi-Söder, C. Schüth, H. Siebner, Low trihalomethane formation during managed aquifer recharge with chlorinated desalinated water, Water 12 (2020) 711, https://doi.org/10.3390/w12030711.

[14] I. Delpla, S. Simard, F. Proulx, J.B. Sérodes, I. Valois, E. Ahmadpour, M. Debia, R. Tardif, S. Haddad, M. Rodriguez, Cumulative impact of swimmers on pool water quality: A full-scale study revealing seasonal and daily variabilities of disinfection by-products, J. Environ. Chem. Eng. 9 (2021), https://doi.org/10.1016/j.jece.2021.106809.

[15] J. Jiang, J. Han, X. Zhang, Nonhalogenated aromatic DBPs in drinking water chlorination: a gap between NOM and halogenated aromatic DBPs, Environ. Sci. Technol. 54 (2020) 1646–1656, https://doi.org/10.1021/acs.est.9b06403.

[16] M. Grote, J.L. Boudenne, J.P. Croué, B.I. Escher, U. von Gunten, J. Hahn, T. Höfer, H. Jenner, J. Jiang, T. Karanfil, M. Khalanski, D. Kim, J. Linders, T. Manasfi, H. Polman, B. Quack, S. Tegtmeier, B. Werschkun, X. Zhang, G. Ziegler, Inputs of disinfection by-products to the marine environment from various industrial activities: comparison to natural production, Water Res. 217 (2022), https://doi.org/10.1016/j.watres.2022.118383.

[17] N. Hong, J. Li, J. Liu, M. Yang, A. Liu, A snapshot on trihalomethanes formation in urban stormwater: Implications for its adequacy as an alternative water resource, J. Environ. Chem. Eng. 10 (2022), 107180, https://doi.org/10.1016/j.jece.2022.107180.

[18] J. Pi, G. Zhu, T. Gong, Y. Lu, Dissolved organic matter derived from aquatic plants in constructed wetlands: characteristics and disinfection byproducts formation, J. Environ. Chem. Eng. 10 (2022), 107991, https://doi.org/10.1016/j.jece.2022.107991.

[19] I. Fisher, G. Kastl, A. Sathasivan, R. Catling, Modelling chlorine residual and trihalomethane profiles in water distribution systems after treatment including pre-chlorination, J. Environ. Chem. Eng. 9 (2021), 105686, https://doi.org/10.1016/j.jece.2021.105686.

[20] S.D. Richardson, M.J. Plewa, To regulate or not to regulate? What to do with more toxic disinfection by-products? J. Environ. Chem. Eng. 8 (2020), 103939 https://doi.org/10.1016/j.jece.2020.103939.

[21] R. Sinha, A.K. Gupta, P.S. Ghosal, A review on trihalomethanes and haloacetic acids in drinking water: Global status, health impact, insights of control and removal technologies, J. Environ. Chem. Eng. 9 (2021) 106511, https://doi.org/10.1016/j.jece.2021.106511.

[22] R.T. Wilkin, S.D. Acree, R.R. Ross, R.W. Puls, T.R. Lee, L.L. Woods, Fifteen-year assessment of a permeable reactive barrier for treatment of chromate and trichloroethylene in groundwater, Sci. Total Environ. 468–469 (2014) 186–194, https://doi.org/10.1016/j.scitotenv.2013.08.056.

[23] S.F. O'Hannesin, R.W. Gillham, Long-term performance of an in situ "Iron Wall" for remediation of VOCs, Ground Water 36 (1998) 164–170, https://doi.org/10.1111/j.1745-6584.1998.tb01077.x.

[24] W.X. Zhang, Nanoscale iron particles for environmental remediation: an overview, J. Nanopart. Res. 5 (2003) 323–332, https://doi.org/10.1023/A:1025520116015.

[25] K. Pandey, S. Sharma, S. Saha, Advances in design and synthesis of stabilized zero-valent iron nanoparticles for groundwater remediation, J. Environ. Chem. Eng. 10 (2022), 107993, https://doi.org/10.1016/j.jece.2022.107993.

[26] N. Munakata, M. Reinhard, Palladium catalysis for the treatment of contaminated waters: a review, in: Physicochem. Groundw. Remediat., Kluwer Academic Publishers, Boston, 2001, pp. 45–71, https://doi.org/10.1007/0-306-46928-6_3.

[27] F.D. Kopinke, K. Mackenzie, R. Köhler, Catalytic hydrodechlorination of groundwater contaminants in water and in the gas phase using Pd/γ-Al2O3, Appl. Catal. B Environ. 44 (2003) 15–24, https://doi.org/10.1016/S0926-3373(03)00006-7.

[28] G.V. Lowry, M. Reinhard, Hydrodehalogenation of 1- to 3-carbon halogenated organic compounds in water using a palladium catalyst and hydrogen gas, Environ. Sci. Technol. 33 (1999) 1905–1910, https://doi.org/10.1021/es980963m.

[29] G.V. Lowry, M. Reinhard, Pd-catalyzed TCE dechlorination in groundwater: solute effects, biological control, and oxidative catalyst regeneration, Environ. Sci. Technol. 34 (2000) 3217–3223, https://doi.org/10.1021/es991416j.

[30] D.M. Cwiertny, S.J. Bransfield, K.J.T. Livi, D.H. Fairbrother, A.L. Roberts, Exploring the influence of granular iron additives on 1,1,1-trichloroethane reduction, Environ. Sci. Technol. 40 (2006) 6837–6843, https://doi.org/10.1021/es060921v.

[31] F. He, D. Zhao, Hydrodechlorination of trichloroethene using stabilized Fe-Pd nanoparticles: Reaction mechanism and effects of stabilizers, catalysts and reaction conditions, Appl. Catal. B Environ. 84 (2008) 533–540, https://doi.org/10.1016/j.apcatb.2008.05.008.

[32] P. Bennett, F. He, D. Zhao, B. Aiken, L. Feldman, In situ testing of metallic iron nanoparticle mobility and reactivity in a shallow granular aquifer, J. Contam. Hydrol. 116 (2010) 35–46, https://doi.org/10.1016/j.jconhyd.2010.05.006.

[33] X. Wang, C. Chen, Y. Chang, H. Liu, Dechlorination of chlorinated methanes by Pd/Fe bimetallic nanoparticles, J. Hazard. Mater. 161 (2009) 815–823, https://doi.org/10.1016/j.jhazmat.2008.04.027.

[34] H.L. Lien, W.X. Zhang, Nanoscale Pd/Fe bimetallic particles: catalytic effects of palladium on hydrodechlorination, Appl. Catal. B Environ. 77 (2007) 110–116, https://doi.org/10.1016/j.apcatb.2007.07.014.

[35] J. Feng, T.T. Lim, Iron-mediated reduction rates and pathways of halogenated methanes with nanoscale Pd/Fe: analysis of linear free energy relationship, Chemosphere 66 (2007) 1765–1774, https://doi.org/10.1016/j.chemosphere.2006.06.068.

[36] N.E. Korte, J.L. Zutman, R.M. Schlosser, L. Liang, B. Gu, Q. Fernando, Field application of palladized iron for the dechlorination of trichloroethene, Waste Manag. 20 (2000) 687–694, https://doi.org/10.1016/S0956-053X(00)00037-4.

[37] C. Schüth, N.A. Kummer, C. Weidenthaler, H. Schad, Field application of a tailored catalyst for hydrodechlorinating chlorinated hydrocarbon contaminants in groundwater, Appl. Catal. B Environ. 52 (2004) 197–203, https://doi.org/10.1016/j.apcatb.2004.03.018.

[38] W.W. Mcnab, R. Ruiz, M. Reinhard, In-situ destruction of chlorinated hydrocarbons in groundwater using catalytic reductive dehalogenation in a reactive well: Testing and operational experiences, Environ. Sci. Technol. 34 (2000) 149–153, https://doi.org/10.1021/es9903936.

[39] M.G. Davie, H. Cheng, G.D. Hopkins, C.A. Lebron, M. Reinhard, Implementing heterogeneous catalytic dechlorination technology for remediating TCE-contaminated groundwater, Environ. Sci. Technol. 42 (2008) 8908–8915, https://doi.org/10.1021/es8014919.

[40] M. Zheng, J. Bao, P. Liao, K. Wang, S. Yuan, M. Tong, H. Long, Electrogeneration of H2 for Pd-catalytic hydrodechlorination of 2,4-dichlorophenol in groundwater, Chemosphere 87 (2012) 1097–1104, https://doi.org/10.1016/j.chemosphere.2012.01.058.

[41] S. Yuan, X. Mao, A.N. Alshawabkeh, Efficient degradation of TCE in groundwater using Pd and electro-generated H2 and O2: a shift in pathway from hydrodechlorination to oxidation in the presence of ferrous ions, Environ. Sci. Technol. 46 (2012) 3398–3405, https://doi.org/10.1021/es204546u.

[42] H. Weiss, B. Daus, P. Fritz, F.D. Kopinke, P. Popp, L. Wünsche, In situ groundwater remediation research in the Bitterfeld region in eastern Germany (SAFIRA), IAHS-AISH Publ. (1998) 443–450.

[43] W.W. McNab, R. Ruiz, Palladium-catalyzed reductive dehalogenation of dissolved chlorinated aliphatics using electrolytically-generated hydrogen, Chemosphere 37 (1998) 925–936, https://doi.org/10.1016/S0045-6535(98)00095-2.

[44] H. Song, E.R. Carraway, Reduction of chlorinated methanes by nano-sized zero-valent iron. Kinetics, pathways, and effect of reaction conditions, Environ. Eng. Sci. 23 (2006) 272–284, https://doi.org/10.1089/ees.2006.23.272.

[45] Y. Han, C. Liu, J. Horita, W. Yan, Trichloroethene hydrodechlorination by Pd-Fe bimetallic nanoparticles: Solute-induced catalyst deactivation analyzed by carbon isotope fractionation, Appl. Catal. B Environ. 188 (2016) 77–86, https://doi.org/10.1016/j.apcatb.2016.01.047.

[46] J. Xiao, Q. Yue, B. Gao, Y. Sun, J. Kong, Y. Gao, Q. Li, Y. Wang, Performance of activated carbon/nanoscale zero-valent iron for removal of trihalomethanes (THMs) at infinitesimal concentration in drinking water, Chem. Eng. J. 253 (2014) 63–72, https://doi.org/10.1016/j.cej.2014.05.030.

[47] E.J. Reardon, Capture and storage of hydrogen gas by zero-valent iron, J. Contam. Hydrol. 157 (2014) 117–124, https://doi.org/10.1016/j.jconhyd.2013.11.007.

[48] P.G. Tratnyek, R.L. Johnson, Nanotechnologies for environmental cleanup, Nano Today 1 (2006) 44–48, https://doi.org/10.1016/S1748-0132(06)70048-2.

[49] R. Focht, J. Vogan, S. O'Hannesin, Field application of reactive iron walls for in-situ degradation of volatile organic compounds in groundwater, Remediation 6 (1996) 81–94, https://doi.org/10.1002/rem.3440060307.

[50] W.X. Zhang, D.W. Elliott, Applications of iron nanoparticles for groundwater remediation, Remediation 16 (2006) 7–21, https://doi.org/10.1002/rem.20078.

[51] M. Elsner, G.L. Couloume, S. Mancini, L. Burns, B.S. Lollar, Carbon isotope analysis to evaluate nanoscale Fe(O) treatment at a chlorohydrocarbon contaminated site, Gr. Water Monit. Remediat 30 (2010) 79–95, https://doi.org/10.1111/j.1745-6592.2010.01294.x.

[52] N.C. Mueller, J. Braun, J. Bruns, M. Černík, P. Rissing, D. Rickerby, B. Nowack, Application of nanoscale zero valent iron (NZVI) for groundwater remediation in Europe, Environ. Sci. Pollut. Res. 19 (2012) 550–558, https://doi.org/10.1007/s11356-011-0576-3.

[53] D.W. Elliott, W.X. Zhang, Field assessment of nanoscale bimetallic particles for groundwater treatment, Environ. Sci. Technol. 35 (2001) 4922–4926, https://doi.org/10.1021/es0108584.

[54] D. O'Carroll, B. Sleep, M. Krol, H. Boparai, C. Kocur, Nanoscale zero valent iron and bimetallic particles for contaminated site remediation, Adv. Water Resour. 51 (2013) 104–122, https://doi.org/10.1016/j.advwatres.2012.02.005.

[55] K.W. Henn, D.W. Waddill, Utilization of nanoscale zero-valent iron for source remediation—a case study, Remediation 16 (2006) 57–77, https://doi.org/10.1002/rem.20081.

[56] K.J. Cantrell, D.I. Kaplan, Zero-valent iron colloid emplacement in sand columns, J. Environ. Eng. 123 (1997) 499–505, https://doi.org/10.1061/(asce)0733-9372(1997)123:5(499).

[57] C. Lebron, M. Reinhard, G. Hopkins, M. Davie, In situ catalytic groundwater treatment using Pd-catalysts and horizontal flow treatment wells, Naval Facilities Engineering Service Center Port Hueneme CA. (2007). https://apps.dtic.mil/sti/pdfs/ADA499385.pdf.

[58] R.W. Gillham, S.F. O'Hannesin, Enhanced degradation of halogenated aliphatics by zero-valent iron, Ground Water 32 (1994).

[59] R.W. Gillham, Cleaning halogenated contaminants from groundwater, (1993) 1–7. https://patents.google.com/patent/US5266213A.

[60] L.J. Matheson, P.G. Tratnyek, Reductive dehalogenation of chlorinated methanes by iron metal, Environ. Sci. Technol. 28 (1994) 2045–2053, https://doi.org/10.1021/es00061a012.

[61] P.J. Novak, L. Daniels, G.F. Parkin, Enhanced dechlorination of carbon tetrachloride and chloroform in the presence of elemental iron and methanosarcina barkeri, methanosarcina thermophila, or methanosaeta concillii, Environ. Sci. Technol. 32 (1998) 1438–1443, https://doi.org/10.1021/es970785h.

[62] T.L. Johnson, M.M. Scherer, P.G. Tratnyek, Kinetics of halogenated organic compound degradation by iron metal, Environ. Sci. Technol. 30 (1996) 2634–2640, https://doi.org/10.1021/es9600901.

[63] J. Feng, T.T. Lim, Pathways and kinetics of carbon tetrachloride and chloroform reductions by nano-scale Fe and Fe/Ni particles: Comparison with commercial micro-scale Fe and Zn, Chemosphere 59 (2005) 1267–1277, https://doi.org/10.1016/j.chemosphere.2004.11.038.

[64] M. Lee, E. Wells, Y.K. Wong, J. Koenig, L. Adrian, H.H. Richnow, M. Manefield, Relative contributions of dehalobacter and zerovalent iron in the degradation of chlorinated methanes, Environ. Sci. Technol. 49 (2015) 4481–4489, https://doi.org/10.1021/es5052364.

[65] X.L. Xuan, X.Z. Li, C. Wang, H. Liu, Effects of key reaction parameters on the reductive dechlorination of chloroform with Pd/Fe0 bimetal in aqueous solution, J. Environ. Sci. Heal. - Part A Toxic. /Hazard. Subst. Environ. Eng. 45 (2010) 464–470, https://doi.org/10.1080/10934520903538608.

[66] J.C. Velázquez, S. Leekumjorn, G.D. Hopkins, K.N. Heck, J.S. McPherson, J.A. Wilkens, B.S. Nave, M. Reinhard, M.S. Wong, High activity and regenerability of a palladium–gold catalyst for chloroform degradation, J. Chem. Technol. Biotechnol. 91 (2016) 2590–2596, https://doi.org/10.1002/jctb.4851.

[67] M.A. Álvarez-Montero, L.M. Gómez-Sainero, M. Martín-Martínez, F. Heras, J.J. Rodriguez, Hydrodechlorination of chloromethanes with Pd on activated carbon catalysts for the treatment of residual gas streams, Appl. Catal. B Environ. 96 (2010) 148–156, https://doi.org/10.1016/j.apcatb.2010.02.012.

[68] M. Martin-Martinez, L.M. Gómez-Sainero, M.A. Alvarez-Montero, J. Bedia, J.J. Rodriguez, Comparison of different precious metals in activated carbon-supported catalysts for the gas-phase hydrodechlorination of chloromethanes, Appl. Catal. B Environ. 132–133 (2013) 256–265, https://doi.org/10.1016/j.apcatb.2012.11.041.

[69] M. Martin-Martinez, J.J. Rodriguez, R.T. Baker, L.M. Gómez-Sainero, Deactivation and regeneration of activated carbon-supported Rh and Ru catalysts in the hydrodechlorination of chloromethanes into light olefins, Chem. Eng. J. 397 (2020), 125479, https://doi.org/10.1016/j.cej.2020.125479.

[70] S. Liu, J.A. Otero, M. Martin-Martinez, D. Rodriguez-Franco, J.J. Rodriguez, L.M. Gómez-Sainero, Understanding hydrodechlorination of chloromethanes, Future Technol., Catal. 10 (2020) 1–38, https://doi.org/10.3390/catal10121462.

[71] R. Muftikian, Q. Fernando, N. Korte, A method for the rapid dechlorination of low molecular weight chlorinated hydrocarbons in water, Water Res. 29 (1995) 2434–2439, https://doi.org/10.1016/0043-1354(95)00102-Q.

[72] S. Ordóñez, H. Sastre, F.V. Díez, Hydrodechlorination of aliphatic organochlorinated compounds over commercial hydrogenation catalysts, Appl. Catal. B Environ. 25 (2000) 49–58, https://doi.org/10.1016/S0926-3373(99)00119-8.

[73] L. Prati, M. Rossi, Reductive catalytic dehalogenation of light chlorocarbons, Appl. Catal. B Environ. 23 (1999) 135–142, https://doi.org/10.1016/S0926-3373(99)00071-5.

[74] N. Chen, R.M. Rioux, L.A.M.M. Barbosa, F.H. Ribeiro, Kinetic and theoretical study of the hydrodechlorination of CH 4- xClx (x = 1-4) compounds on palladium, Langmuir 26 (2010) 16615–16624, https://doi.org/10.1021/la1020753.

[75] L.M. Gómez-Sainero, X.L. Seoane, E. Tijero, A. Arcoya, Hydrodechlorination of carbon tetrachloride to chloroform in the liquid phase with a Pd/carbon catalyst.

Study of the mass transfer steps, Chem. Eng. Sci. 57 (2002) 3565–3574, https://doi.org/10.1016/S0009-2509(02)00250-6.

[76] D.A. Dodson, H.F. Rase, Methylene Chloride from chloroform by hydrochlorination, Ind. Eng. Chem. Prod. Res. Dev. 17 (1978) 236–240, https://doi.org/10.1021/i360067a012.

[77] J.C. Velázquez, S. Leekumjorn, Q.X. Nguyen, Y.-L. Fang, K.N. Heck, G.D. Hopkins, M. Reinhard, M.S. Wong, Chloroform hydrodechlorination behavior of alumina-supported Pd and PdAu catalysts, AIChE J. 59 (2013) 4474–4482, https://doi.org/10.1002/aic.14250.

[78] T. Mori, K. Hirose, T. Kikuchi, J. Kubo, Y. Morikawa, Formation of higher hydrocarbons from chloromethanes via hydrodechlorination over Pd/SiO2 catalyst, J. Jpn. Pet. Inst. 45 (2002) 321–324, https://doi.org/10.1627/jpi.45.321.

[79] L. Xu, Y. Yao, A. Khan, M. Mavrikakis, Chloroform hydrodechlorination over Palladium-Gold catalysts: a first-principles DFT study, ChemCatChem 8 (2016) 1739–1746, https://doi.org/10.1002/cctc.201600144.

[80] R.U. Meckenstock, B. Morasch, C. Griebler, H.H. Richnow, Stable isotope fractionation analysis as a tool to monitor biodegradation in contaminated aquifers, J. Contam. Hydrol. 75 (2004) 215–255, https://doi.org/10.1016/j.jconhyd.2004.06.003.

[81] M. Bill, C. Schüth, J.A.C. Barth, R.M. Kalin, Carbon isotope fractionation during abiotic reductive dehalogenation of trichloroethene (TCE), Chemosphere 44 (2001) 1281–1286, https://doi.org/10.1016/S0045-6535(00)00274-5.

[82] M. Elsner, L. Zwank, D. Hunkeler, R.P. Schwarzenbach, A new concept linking observable stable isotope fractionation to transformation pathways of organic pollutants, Environ. Sci. Technol. 39 (2005) 6896–6916, https://doi.org/10.1021/es0504587.

[83] F. Breider, D. Hunkeler, Investigating chloroperoxidase-catalyzed formation of chloroform from humic substances using stable chlorine isotope analysis, Environ. Sci. Technol. 48 (2014) 1592–1600, https://doi.org/10.1021/es403879e.

[84] A. Cincinelli, F. Pieri, Y. Zhang, M. Seed, K.C. Jones, Compound specific isotope analysis (CSIA) for chlorine and bromine: a review of techniques and applications to elucidate environmental sources and processes, Environ. Pollut. 169 (2012) 112–127, https://doi.org/10.1016/j.envpol.2012.05.006.

[85] D. Hunkeler, T. Laier, F. Breider, O.S. Jacobsen, Demonstrating a natural origin of chloroform in groundwater using stable carbon isotopes, Environ. Sci. Technol. 46 (2012) 6096–6101, https://doi.org/10.1021/es204585d.

[86] N. Jendrzejewski, H.G.M. Eggenkamp, M.L. Coleman, Characterisation of chlorinated hydrocarbons from chlorine and carbon isotopic compositions: Scope of application to environmental problems, Appl. Geochem. 16 (2001) 1021–1031, https://doi.org/10.1016/S0883-2927(00)00083-4.

[87] T.C. Schmidt, R.U. Meckenstock, S.B. Haderlein, L. Zwank, M. Elsner, M. Berg, Compound-specific stable isotope analysis of organic contaminants in natural environments: a critical review of the state of the art, prospects, and future challenges, Anal. Bioanal. Chem. 378 (2004) 283–300, https://doi.org/10.1007/s00216-003-2350-y.

[88] E.M. van Warmerdam, S.K. Frape, R. Aravena, R.J. Drimmie, H. Flatt, J.A. Cherry, Stable chlorine and carbon isotope measurements of selected chlorinated organic solvents, Appl. Geochem. 10 (1995) 547–552, https://doi.org/10.1016/0883-2927(95)00025-9.

[89] S.K. Hirschorn, M.J. Dinglasan, M. Elsner, S.A. Mancini, G. Lacrampe-Couloume, E.A. Edwards, B. Sherwood Lollar, Pathway dependent isotopic fractionation during aerobic biodegradation of 1,2-dichloroethane, Environ. Sci. Technol. 38 (2004) 4775–4781, https://doi.org/10.1021/es049920y.

[90] J. Palau, P. Jamin, A. Badin, N. Vanhecke, B. Haerens, S. Brouyère, D. Hunkeler, Use of dual carbon-chlorine isotope analysis to assess the degradation pathways of 1,1,1-trichloroethane in groundwater, Water Res. 92 (2016) 235–243, https://doi.org/10.1016/j.watres.2016.01.057.

[91] J. Palau, S. Cretnik, O. Shouakar-Stash, M. Höche, M. Elsner, D. Hunkeler, C and Cl isotope fractionation of 1,2-dichloroethane displays unique δ13C/δ37Cl patterns for pathway identification and reveals surprising C-Cl bond involvement in microbial oxidation, Environ. Sci. Technol. 48 (2014) 9430–9437, https://doi.org/10.1021/es5031917.

[92] J. Palau, O. Shouakar-Stash, S. Hatijah Mortan, R. Yu, M. Rosell, E. Marco-Urrea, D.L. Freedman, R. Aravena, A. Soler, D. Hunkeler, Hydrogen isotope fractionation during the biodegradation of 1,2-dichloroethane: Potential for pathway identification using a multi-element (C, Cl, and H) isotope approach, Environ. Sci. Technol. 51 (2017) 10526–10535, https://doi.org/10.1021/acs.est.7b02906.

[93] J. Palau, O. Shouakar-Stash, D. Hunkeler, Carbon and chlorine isotope analysis to identify abiotic degradation pathways of 1,1,1-trichloroethane, Environ. Sci. Technol. 48 (2014) 14400–14408, https://doi.org/10.1021/es504252z.

[94] C. Schüth, M. Bill, J.A.C. Barth, G.F. Slater, R.M. Kalin, Carbon isotope fractionation during reductive dechlorination of TCE in batch experiments with iron samples from reactive barriers, J. Contam. Hydrol. 66 (2003) 25–37, https://doi.org/10.1016/S0169-7722(03)00026-3.

[95] M. Elsner, M. Chartrand, N. VanStone, G. Lacrampe Couloume, B. Sherwood Lollar, Identifying abiotic chlorinated ethene degradation: Characteristic isotope patterns in reaction products with nanoscale zero-valent iron, Environ. Sci. Technol. 42 (2008) 5963–5970, https://doi.org/10.1021/es8001986.

[96] K. Sakaguchi-Söder, J. Jager, H. Grund, F. Matthäus, C. Schüth, Monitoring and evaluation of dechlorination processes using compound-specific chlorine isotope analysis, Rapid Commun. Mass Spectrom. 21 (2007) 3077–3084, https://doi.org/10.1002/rcm.3170.

[97] W.A. Arnold, J. Bolotin, U. Von Gunten, T.B. Hofstetter, Evaluation of functional groups responsible for chloroform formation during water chlorination using compound specific isotope analysis, Environ. Sci. Technol. 42 (2008) 7778–7785, https://doi.org/10.1021/es800399a.

[98] C.C.H. Chan, S.O.C. Mundle, T. Eckert, X. Liang, S. Tang, G. Lacrampe-Couloume, E.A. Edwards, B. Sherwood Lollar, Large carbon isotope fractionation during biodegradation of chloroform by dehalobacter cultures, Environ. Sci. Technol. 46 (2012) 10154–10160, https://doi.org/10.1021/es3010317.

[99] A.S. Ojeda, E. Phillips, B. Sherwood Lollar, Multi-element (C, H, Cl, Br) stable isotope fractionation as a tool to investigate transformation processes for halogenated hydrocarbons, Environ. Sci. Process. Impacts 22 (2020) 567–582, https://doi.org/10.1039/c9em00498j.

[100] C. Torrentó, J. Palau, D. Rodríguez-Fernández, B. Heckel, A. Meyer, C. Domènech, M. Rosell, A. Soler, M. Elsner, D. Hunkeler, Carbon and chlorine isotope fractionation patterns associated with different engineered chloroform transformation reactions, Environ. Sci. Technol. 51 (2017) 6174–6184, https://doi.org/10.1021/acs.est.7b00679.

[101] D. Rodríguez-Fernández, C. Torrentó, J. Palau, M. Marchesi, A. Soler, D. Hunkeler, C. Domènech, M. Rosell, Unravelling long-term source removal effects and chlorinated methanes natural attenuation processes by C and Cl stable isotopic patterns at a complex field site, Sci. Total Environ. 645 (2018) 286–296, https://doi.org/10.1016/j.scitotenv.2018.07.130.

[102] J.M. Soder-Walz, C. Torrentó, C. Algora, K. Wasmund, P. Cortés, A. Soler, T. Vicent, M. Rosell, E. Marco-Urrea, Trichloromethane dechlorination by a novel Dehalobacter sp. strain 8 M reveals a third contrasting C and Cl isotope fractionation pattern within this genus, Sci. Total Environ. 813 (2021), 152659, https://doi.org/10.1016/j.scitotenv.2021.152659.

[103] A. Gafni, C. Lihl, F. Gelman, M. Elsner, A. Bernstein, δ13C and δ37Cl isotope fractionation to characterize aerobic vs anaerobic degradation of trichloroethylene, Environ. Sci. Technol. Lett. 5 (2018) 202–208, https://doi.org/10.1021/acs.estlett.8b00100.

[104] A.S. Ojeda, E. Phillips, S.A. Mancini, B.S. Lollar, Sources of uncertainty in biotransformation mechanistic interpretations and remediation studies using CSIA, Anal. Chem. 91 (2019) 9147–9153, https://doi.org/10.1021/acs.analchem.9b01756.

[105] I. Yankelzon, T. Englman, A. Bernstein, H. Siebner, Z. Ronen, F. Gelman, Multi-elemental C-Br-Cl isotope analysis for characterizing biotic and abiotic transformations of 1-bromo-2-chloroethane (BCE), Environ. Sci. Pollut. Res. (2020), https://doi.org/10.1007/s11356-020-08870-6.

[106] C. Audí-Miró, S. Cretnik, N. Otero, J. Palau, O. Shouakar-Stash, A. Soler, M. Elsner, Cl and C isotope analysis to assess the effectiveness of chlorinated ethene degradation by zero-valent iron: Evidence from dual element and product isotope values, Appl. Geochem. 32 (2013) 175–183, https://doi.org/10.1016/j.apgeochem.2012.08.025.

[107] C. Wiegert, C. Aeppli, T. Knowles, H. Holmstrand, R. Evershed, R.D. Pancost, J. Macháčková, Ö. Gustafsson, Dual carbon-chlorine stable isotope investigation of sources and fate of chlorinated ethenes in contaminated groundwater, Environ. Sci. Technol. 46 (2012) 10918–10925, https://doi.org/10.1021/es3016843.

[108] B. Heckel, E. Phillips, E. Edwards, B. Sherwood Lollar, M. Elsner, M.J. Manefield, M. Lee, Reductive dehalogenation of trichloromethane by two different dehalobacter restrictus strains reveal opposing dual element isotope effects, Environ. Sci. Technol. 53 (2019) 2332–2343, https://doi.org/10.1021/acs.est.8b03717.

[109] S. Cretnik, K.A. Thoreson, A. Bernstein, K. Ebert, D. Buchner, C. Laskov, S. Haderlein, O. Shouakar-Stash, S. Kliegman, K. McNeill, M. Elsner, Reductive dechlorination of TCE by chemical model systems in comparison to dehalogenating bacteria: Insights from dual element isotope analysis (13C/12C, 37Cl/35Cl), Environ. Sci. Technol. 47 (2013) 6855–6863, https://doi.org/10.1021/es400107n.

[110] H. Penning, S.R. Sørensen, A.H. Meyer, J. Aamand, M. Elsner, C, N, and H isotope fractionation of the herbicide lsoproturon reflects different microbial transformation pathways, Environ. Sci. Technol. 44 (2010) 2372–2378, https://doi.org/10.1021/es9031858.

[111] Y. Abe, R. Aravena, J. Zopfi, O. Shouakar-Stash, E. Cox, J.D. Roberts, D. Hunkeler, Carbon and chlorine isotope fractionation during aerobic oxidation and reductive dechlorination of vinyl chloride and cis-1, 2-dichloroethene, Environ. Sci. Technol. 43 (2009) 101–107, https://doi.org/10.1021/es801759k.

[112] F.D. Bergmann, N.M.F.H. Abu Laban, A.H. Meyer, M. Elsner, R.U. Meckenstock, Dual (C, H) isotope fractionation in anaerobic low molecular weight (poly) aromatic hydrocarbon (PAH) degradation: potential for field studies and mechanistic implications, Environ. Sci. Technol. 45 (2011) 6947–6953, https://doi.org/10.1021/es201096j.

[113] J. Renpenning, S. Keller, S. Cretnik, O. Shouakar-Stash, M. Elsner, T. Schubert, I. Nijenhuis, Combined C and Cl isotope effects indicate differences between corrinoids and enzyme (Sulfurospirillum multivorans PceA) in reductive dehalogenation of tetrachloroethene, but not trichloroethene, Environ. Sci. Technol. 48 (2014) 11837–11845, https://doi.org/10.1021/es503306g.

[114] J. Zimmermann, L.J.S. Halloran, D. Hunkeler, Tracking chlorinated contaminants in the subsurface using compound-specific chlorine isotope analysis: a review of principles, current challenges and applications, Chemosphere 244 (2020), 125476, https://doi.org/10.1016/j.chemosphere.2019.125476.

[115] K. Kuntze, H. Eisenmann, H.-H. Richnow, A. Fischer, Compound-specific stable isotope analysis (CSIA) for evaluating degradation of organic pollutants: An overview of field case studies, in: Anaerob. Util. Hydrocarb. Oils, Lipids, Springer International Publishing, Cham, 2019: pp. 1–39. https://doi.org/10.1007/978-3-319-33598-8_23–1.

[116] H.H. Richnow, E. Annweiler, W. Michaelis, R.U. Meckenstock, Microbial in situ degradation of aromatic hydrocarbons in a contaminated aquifer monitored by

carbon isotope fractionation, J. Contam. Hydrol. 65 (2003) 101–120, https://doi.org/10.1016/S0169-7722(02)00233-4.

[117] C. Torrentó, C. Audí-Miró, G. Bordeleau, M. Marchesi, M. Rosell, N. Otero, A. Soler, The use of alkaline hydrolysis as a novel strategy for chloroform remediation: the feasibility of using construction wastes and evaluation of carbon isotopic fractionation, Environ. Sci. Technol. 48 (2014) 1869–1877, https://doi.org/10.1021/es403838t.

[118] C. Schüth, M. Reinhard, Hydrodechlorination and hydrogenation of aromatic compounds over palladium on alumina in hydrogen-saturated water, Appl. Catal. B Environ. 18 (1998) 215–221, https://doi.org/10.1016/S0926-3373(98)00037-X.

[119] H. Prommer, L.H. Aziz, N. Bolaño, H. Taubald, C. Schüth, Modelling of geochemical and isotopic changes in a column experiment for degradation of TCE by zero-valent iron 97 (2008) 13–26, https://doi.org/10.1016/j.jconhyd.2007.11.003.

[120] B.A. Asfaw, K. Sakaguchi-Söder, A. Bernstein, H. Siebner, C. Schüth, Optimization of compound-specific chlorine stable isotope analysis of chloroform using the Taguchi design of experiments, Rapid Commun. Mass Spectrom. 34 (2020) 1–7, https://doi.org/10.1002/rcm.8922.

[121] I.D. Clark, P. Fritz, Environmental Isotopes in Hydrogeology, CRC Press, New York, 1997, https://doi.org/10.1201/9781482242911.

[122] D. Buchner, B. Jin, K. Ebert, M. Rolle, M. Elsner, S.B. Haderlein, Experimental determination of isotope enrichment factors - Bias from mass removal by repetitive sampling, Environ. Sci. Technol. 51 (2017) 1527–1536, https://doi.org/10.1021/acs.est.6b03689.

[123] D. York, Least squares fitting of a straight line with correlated errors, Earth Planet. Sci. Lett. 5 (1968) 320–324, https://doi.org/10.1016/S0012-821X(68)80059-7.

[124] P. Vermeesch, Geoscience Frontiers IsoplotR: a free and open toolbox for geochronology, Geosci. Front 9 (2018) 1479–1493, https://doi.org/10.1016/j.gsf.2018.04.001.

[125] D. Rodríguez-Fernández, B. Heckel, C. Torrentó, A. Meyer, M. Elsner, D. Hunkeler, A. Soler, M. Rosell, C. Domènech, Dual element (C-Cl) isotope approach to distinguish abiotic reactions of chlorinated methanes by Fe(0) and by Fe(II) on iron minerals at neutral and alkaline pH, Chemosphere 206 (2018) 447–456, https://doi.org/10.1016/j.chemosphere.2018.05.036.

[126] M. Löffler, S. Kümmel, C. Vogt, H.H. Richnow, H2 kinetic isotope fractionation superimposed by equilibrium isotope fractionation during hydrogenase activity of D. Vulgaris Strain Miyazaki, Front. Microbiol. 10 (2019), https://doi.org/10.3389/fmicb.2019.01545.

[127] T. Kuder, B.M. Van Breukelen, M. Vanderford, P. Philp, 3D-CSIA: carbon, chlorine, and hydrogen isotope fractionation in transformation of TCE to ethene by a dehalococcoides culture, Environ. Sci. Technol. 47 (2013) 9668–9677, https://doi.org/10.1021/es400463p.

[128] B.M. Van Breukelen, H.A.A. Thouement, P.E. Stack, M. Vanderford, P. Philp, T. Kuder, Modeling 3D-CSIA data: carbon, chlorine, and hydrogen isotope fractionation during reductive dechlorination of TCE to ethene, J. Contam. Hydrol. 204 (2017) 79–89, https://doi.org/10.1016/j.jconhyd.2017.07.003.

[129] M. Rostkowski, H.K.V. Schürner, A. Sowińska, L. Vasquez, M. Przydacz, M. Elsner, A. Dybala-Defratyka, Isotope effects on the vaporization of organic compounds from an aqueous solution–Insight from experiment and computations, J. Phys. Chem. B 125 (2021) 13868–13885, https://doi.org/10.1021/acs.jpcb.1c05574.

[130] A. Horst, G. Lacrampe-Couloume, Isotope fractionation (2H/1H, 13C/12C, 37Cl/35Cl) in trichloromethane and trichloroethene caused by partitioning between gas phase and water, Environ. Sci. Process. Impacts 22 (2020) 617–626, https://doi.org/10.1039/c9em00583h.

[131] B. Heckel, D. Rodríguez-Fernández, C. Torrentó, A. Meyer, J. Palau, C. Domènech, M. Rosell, A. Soler, D. Hunkeler, M. Elsner, Compound-specific chlorine isotope analysis of tetrachloromethane and trichloromethane by gas chromatography-isotope ratio mass spectrometry vs gas chromatography-quadrupole mass spectrometry: method development and evaluation of precision and trueness, Anal. Chem. 89 (2017) 3411–3420, https://doi.org/10.1021/acs.analchem.6b04129.

[132] S. Perathoner, G. Centi, S. Gross, E.J. Hensen, Science and Technology Roadmap on Catalysis for Europe, ERIC aisbl Pub.,Bruxelles(Belgium), 2016. https://www.euchems.eu/roadmap-on-catalysis-for-europe/.

[133] P. Lanzafame, S. Perathoner, G. Centi, S. Gross, E.J.M. Hensen, Grand challenges for catalysis in the science and technology roadmap on catalysis for Europe: Moving ahead for a sustainable future, Catal. Sci. Technol. 7 (2017) 5182–5194, https://doi.org/10.1039/c7cy01067b.